# Time-resolved imaging of microscale dynamics in laser drying of silicon wafers

Zhipeng Wu, Xi Huang, Wanting Sun, Haoyu Dong, Aofei Mao, Bai Cui, Jean-François Silvain, Xinwei Wang, Yongfeng Lu

# Time-resolved imaging of microscale dynamics in laser drying of silicon wafers

Zhipeng Wu [a], Xi Huang [a], Wanting Sun [a], Haoyu Dong [a], Aofei Mao [a], Bai Cui [b], Jean-François Silvain [a c], Xinwei Wang [d], Yongfeng Lu [a]

[a] *Department of Electrical and Computer Engineering, University of Nebraska Lincoln, Nebraska, USA*
[b] *Department of Mechanical and Materials Engineering, University of Nebraska Lincoln, Nebraska, USA*
[c] *CNRS, University of Bordeaux, Bordeaux I.N.P., ICMCB, UMR 5026, F-33608 Pessac, France*
[d] *Department of Mechanical Engineering, Iowa State University, Iowa, USA*

**Abstract :** Surface drying plays a critical role in wafer fabrication in microelectronics, primarily on eliminating watermarks. Spin drying, isopropanol alcohol (IPA) drying, and Marangoni drying are the most commonly used methods, but they have drawbacks such as high risk of water stains, safety hazards, environmental concerns, and energy inefficiency. Hence, there is a continuous demand for fast, efficient, chemical-free, and energy-efficient wafer drying processes. This study explored the use of nanosecond (ns) laser pulses for laser-induced sub-surface evaporation as a promising alternative for surface drying. By adjusting the laser fluence, clean and dry silicon (Si) substrates can be obtained without any stain or damage. Large-area laser drying was also demonstrated. Time-resolved imaging was employed to investigate the drying dynamics after the interaction between the laser pulses and the substrates. It was observed that the deposited water droplet films expand, detach from the substrates, and eject into the air after excimer laser pulses. Moreover, the study examined the influence of substrate conditions on laser drying, including surface roughness and hydrophilicity. The effectiveness of laser drying was evaluated on various substrates, including stainless steels (polished/mirror polished) and glasses. Pulsed lasers demonstrate the ability to dry chemical solutions, such as 35 g/L NaCl, in addition to pure water. These findings show the potential of using ns pulsed lasers as a versatile and environmentally friendly drying tool for various solution and substrate types.

## 1. Introduction

Watermarks (stains) are of significant concern during the drying process in microelectronics [1]. Common manufacturing processes involve transportation of dissolved or suspended chemical species with processing liquid [2], which can leave behind residual liquid on surfaces. To eliminate these residuals, a common approach is to rinse the substrates with water, or a specialized solvent followed by surface drying [2–4]. The drying process plays a significant role in determining surface quality and production yield, as insufficient drying can lead to the formation of undesired deposits of soluble or suspended contaminants [2,5]. This issue is particularly concerning in integrated circuit manufacturing, where increasing pattern density, larger wafer sizes, and shrinking pattern sizes demand meticulous drying techniques [6]. The presence of contaminants on substrate surfaces during the drying process can be attributed to two factors: 1) adsorption of dissolved or suspended chemical species onto the surface when the substrate is in contact with the liquid, and 2) deposition resulting from evaporation, where non-volatile contaminants remain on the surfaces as the liquid transitions to the gas phase [2]. Addressing these factors is crucial to ensure clean and perfect surfaces.

Spin drying, Isopropanol alcohol (IPA) drying, and Marangoni drying are the commonly used methods in wafer drying. Spin drying [5,7,8] utilizes the centrifugal force generated by the high-speed rotation of wafers to remove water. While this method is simple and fast, it still leads to issues such as droplet back splash, increased evaporation rate [9,10], and the potential recontamination of the wafer surface with particles and aerosols due to the mechanical motion of the dryer [1]. In

* Corresponding authors.
*E-mail addresses:* xwang3@iastate.edu (X. Wang), ylu2@unl.edu (Y. Lu).
[1] Zhipeng Wu and Xi Huang contributed equally to this work.

IPA drying [11–14], wet wafers are exposed to a hot IPA vapor that displaces water from the wafer surface. The IPA subsequently evaporates as the wafer cools. Marangoni drying [3,15–18] is a more complex process in which a wafer is gradually withdrawn from water into a vapor mixture of IPA and nitrogen. A surface tension gradient created by this process causes water on the wafer surface to be pulled back into the water body, resulting in a moisture-free surface. However, both the IPA and Marangoni processes consume significant amounts of IPA and energy, making them economically and environmentally unfriendly. Furthermore, the high operating temperatures involved in both processes raise safety concerns [4]. As a result, there is a growing need for alternative drying methods that are more efficient, cost-effective, and environmentally friendly. Research efforts have been focused on developing innovative techniques that minimize IPA and energy consumption, while ensuring effective drying and maintaining safety standards. By addressing these challenges, the microelectronics industry can benefit from more sustainable and efficient wafer drying processes.

In this study, we investigated the use of nanosecond (ns) lasers for laser-induced sub-surface evaporation as a promising alternative for surface drying. To our best knowledge, there have been limited research efforts [19] on laser drying. Although laser wafer drying is derived from laser cleaning [20–25], which has been systematically studied and applied for decades, notable differences exist between the two processes. Laser cleaning primarily focuses on using high-energy photons to break chemical bonds and using laser-induced surface vibration to detach nanoscale particulates [25]. In contrast, laser drying emphasizes the creation of sub-surface superheating and explosive evaporation [26]. The resulting high vapor pressure enables the ejection of liquids [27,28], capable of overcoming surface tension and viscous forces needed for wafer drying. Since the laser fluence (energy density) required for laser drying is lower than that needed for laser cleaning, laser-induced surface damage is unlikely to be an issue based on our previous investigations [29–31]. In this study, we successfully obtained clean Si surfaces without any stains or damage by adjusting laser fluence. Large-area laser drying was also demonstrated. Time-resolved imaging was employed to investigate the drying dynamics after the interaction between the laser pulses and the substrates. It was observed that the deposited water droplet films expand, detach from substrates, and are ejected into the air after the laser pulses. Moreover, the study examined how laser drying is influenced by substrate conditions, including surface roughness and hydrophilicity. The effectiveness of this laser drying technique was evaluated on various substrates, including stainless steels (SS) 316 (polished/mirror polished) and glasses. Moreover, the drying technique demonstrated the ability to dry solutions, such as 35 g/L NaCl, expanding its versatility beyond pure water. These findings highlight the potential of ns pulsed lasers as a versatile and environmentally friendly drying method for various substrate and solution types.

## 2. Experiments

### 2.1. Substrate preparation

Silicon (Si) wafers (SKU#1196, Phos Dopant, CZ growth, Wafer World, Inc.) with a diameter of 100 mm and a thickness of 0.5 mm were employed as the primary substrate in this study. The Si wafers were cut into 12.5 × 12.5 $mm^2$ and ultrasonically cleaned in pure ethanol (200 proof, anhydrous, ≥99.5 %) for 5 min. To remove the native oxide layer, the cleaned substrates were dipped in a 2 % vol. hydrofluoric acid (HF) aqueous solution for 2 min at room temperature, and then thoroughly rinsed with deionized (DI) water. To investigate the influence of surface roughness on laser drying, the cleaned Si wafers were textured using a femtosecond (fs) laser (Amplitude Inc, Tangor) with a wavelength of 1030 nm, controlled by a galvanometer scanner (SCANLAB GmbH). The fs laser was focused on the Si wafers and scanned at a speed of 1 m/s with a 408-fs pulse duration and 330 kHz frequency for 4, 16 and 48 scan passes, respectively. The spot diameter, laser power, and pitch distance of the fs-laser texturing were set at 30 μm, 14 W, and 60 μm, respectively. The fs-laser-textured Si wafers were then chemically modified to tune the hydrophilicity. The modified Si wafers were then dried in an oven at 100 °C. Other substrates were also used to evaluate the effectiveness of laser drying, including commercial stainless steel (SS) 316 plates (OnlineMetals.com), which were cut into dimensions of 10 × 10 × 1 $mm^3$, and glass substrates (Sail Brand) with dimensions of 22 × 26 × 0.5 $mm^3$. The substrates were ultrasonically cleaned in pure ethanol for 5 min before liquid deposition.

### 2.2. Water droplet film deposition

A mist humidifier (LEVOIT) with a mist speed flow of 180.5 mL/h was used to deposit liquid films onto substrates. The deposition time was 10 sec. As shown in **Figure S1**, the mist passed through a flexible tube with an inner diameter of 8 mm and a diffuser head with a diameter of 50 mm, and reached a substrate surface which was placed 10 mm below the diffuser. The room temperature and humidity were kept at 23 °C and 23 %, respectively. High-purity water (Thermo Scientific™ NERL™) and 35 g/L NaCl solution, which was made by dissolving NaCl (Fisher Science Education™) in the high purity water, were employed in this study. To clarify, the term "water droplet film" throughout this paper refers to the presence of numerous water droplets (dis-continuous or semi-continuous water films) on substrate surfaces during laser drying. Typical water droplet distributions on different surfaces were shown in **Figure S1**. These droplet distributions indicate that they are uniformly deposited by the mist humidifier on all surfaces tested. However, the size and shape of the deposited droplets vary on different substrates, due to differences in surface tension. On the Si surface with the HF treatment, the droplets exhibit a round shape with diameters typically ranging from 20 to 40 μm. Without the HF treatment, the droplets on the Si surface are larger, with diameters ranging from 100 to 200 μm. On other substrates, the droplets do not have a round shape. On SS and glasses, the droplets appear to form a semi-continuous water film.

### 2.3. Experimental setup of laser drying and time-resolved imaging

The experiment setup for laser drying and time-resolved imaging is shown in Fig. 1. A KrF excimer laser (COMPex Pro 205F, 248 nm, 20 ns pulse duration, maximum average power 30 W, repetition rate 1 Hz, spot size of 50 $mm^2$ at output) was used to dry water from the Si wafers. To obtain a homogenized excimer laser beam, two identical micro-lens arrays (MLAs) were placed in parallel with a distance of 6 cm to segment the incident laser beam into an array of beamlets. The homogenizer MLAs 1 and 2 were both made of fused silica with a dimension of 20 × 20 $mm^2$ and 0.8 mm pitches. The identical focus length of the two MLAs is 206.5 mm with the same numerical aperture of 0.0019. A lens with a focal length of 600 mm was utilized to converge the beamlets to overlap on the Si wafer [32]. The homogenized excimer laser beam was focused and has a square spot size of about 3.7 × 2.7 $mm^2$ on the sample surface.

For time-resolved imaging, a Q-switched Nd:YAG laser operating at 532 nm (Continuum, Powerlite Precision II 8010) with a pulse duration of 6 ns and a pulse energy of 20 mJ was introduced in parallel to the sample surface during the drying processing by the excimer laser pulses. The Nd:YAG laser was focused at a distance of approximately 10 cm after the excimer laser spot, resulting in a spot diameter of 4 mm in the drying area. To capture the green light (532 nm) scattered by ejected water clusters from substrates during laser drying, a 512 × 512-pixel intensified charge-coupled device (ICCD) (Andor Tech., iStar, DH-712) with a gate width of 1 μs and a multiple channel plate (MCP) gain of 20 was utilized. The excimer laser, Nd:YAG laser, and ICCD were synchronized by a digital delay generator (DDG) (Stanford Research System DG535) with a delay resolution of 5 ps. A pulse generator (Quantum Composers 9514) was used to generate two TTL signals to trigger the Nd:YAG laser. The detailed time sequence for all events is shown in

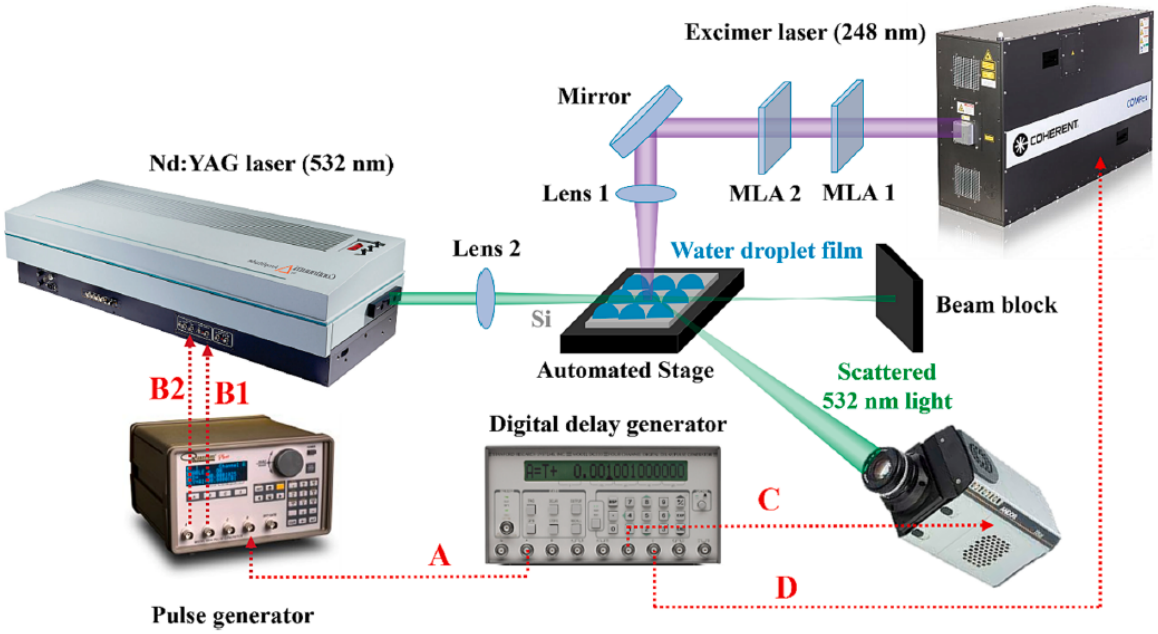


**Fig. 1.** Schematic of the laser drying system using the excimer laser and time-resolved imaging captured by the scattered green light (532 nm) from the Nd:YAG laser.

Figure S2. By precisely controlling the delay among the excimer laser, the Nd:YAG laser, and the ICCD, we obtained the light scattering images of the water clusters ejected from the substrates at various delaying times ranging from 0 μs to 20 ms. This allowed us to study the temporal evolution of drying dynamics in detail.

### 2.4. Characterization

Characterization of the Si surfaces after laser drying was conducted using an environmental scanning electron microscope (SEM) (FEI Quanta 200). A Thermo Fisher K-Alpha X-ray photoelectron spectroscopy (XPS) with an Al K-Alpha X-ray source (1486.68 eV) and a spot size of 40 μm was used to analyze the atomic ratios of oxygen on the Si surfaces after laser drying. Contact angles of the substrates were measured through observing a liquid droplet of 5 μL on the surfaces using a standard goniometer (Ramé-Hart Instrument Co., Model 250-U1). Surface roughness and morphology of the fs textured Si wafer were measured using a NewView 8000 3D optical surface profiler (Zygo Corporation).

## 3. Results and discussions

### 3.1. Laser drying on Si wafer with different laser fluences

In this study, we successfully obtained clean Si substrates without any stains or damage by adjusting the laser fluence during laser drying, as shown in Fig. 2. Fig. 2**a** shows the photographs of a Si wafer with a water droplet film being dried by a single pulse of excimer laser with a fluence of 0.507 J/cm$^2$. It should be noted that due to the multiple reflections between the MLAs, a "ghost" spot appeared next to the main laser spot. The major laser fluence is concentrated in the main laser spot, as shown in Figure S3. The surface oxide layer was initially removed using HF aqueous solution. Therefore, the Si surface became hydrophobic with a contact angle of 77.5° (Fig. 2**b**) due to the adsorbed H and $CH_x$ groups [33]. Water droplets with a thickness of approximately 20 μm were deposited on the Si wafer. After a single excimer laser pulse, a rectangular region devoid of the water droplet film was observed on the surface, indicating the successful removal. In the absence of laser irradiation, evaporation of the water droplets in air left water stains on the surface, even if the pure water was used, as shown in Fig. 2**c**. The dissolved oxygen in the air can lead to the oxidation of the Si surface. The hydrated silicon oxide formed would remain as water stains after natural evaporation [34]. When the applied laser fluence was 0.351 J/cm$^2$, the pulse energy was not sufficient to remove all the liquid, leaving smaller droplets and, consequently, smaller stains on the surface. In comparison, when the excimer laser fluence was increased to 0.726 J/cm$^2$, damage was observed on the Si surface after the laser drying. The focusing effect caused by the convex shapes of the droplets led to a significantly lower damage threshold for the Si surface deposited with a water droplet film. The damage threshold [35] for the Si surface without a water droplet film was reported to be approximately 1.3 J/cm$^2$. By setting the excimer laser fluence to 0.507 J/cm$^2$, a clean surface without stains or damage was achieved. XPS was applied to analyze the variation in oxygen atomic ratio during the drying process. The O1s peaks of the XPS spectra are shown in Figure S4. As shown in Fig. 2**d**, the oxygen atomic ratio of the non-processed Si wafer was 7.66 % with the oxide layer removed. After drying in open air (no laser), the oxygen atomic ratio increased to 9.26 % due to the formation of water stains. With the excimer laser fluence of 0.351 J/cm$^2$, the oxygen atomic ratio fell between those of the Si wafer before and after laser drying in air, indicating an incomplete drying. When the excimer laser fluence was set to 0.507 J/cm$^2$, the oxygen atomic ratio was 7.52 %, which is close to that of the non-processed Si surface, indicating an effective drying process. As the excimer laser fluence increased to 0.726 J/cm$^2$, the oxygen content rose to 10.53 %, indicating the incorporation of oxygen in the damaged or melted region on the Si surface [36,37]. Moreover, a large drying process on an area of 12.5 × 3.7 mm$^2$ was demonstrated by moving an automated stage, as shown in Fig. 2**e**.

### 3.2. Drying dynamics observed through time-resolve imaging

To investigate the drying dynamics, a Q-switched Nd:YAG laser was utilized to initiate optical scattering on the ejected water clusters caused by the explosive evaporation during laser drying. By synchronizing the excimer laser pulse, Nd:YAG laser pulse, and the ICCD, the drying dynamics of the water droplet films were observed, as shown in Fig. 3. The

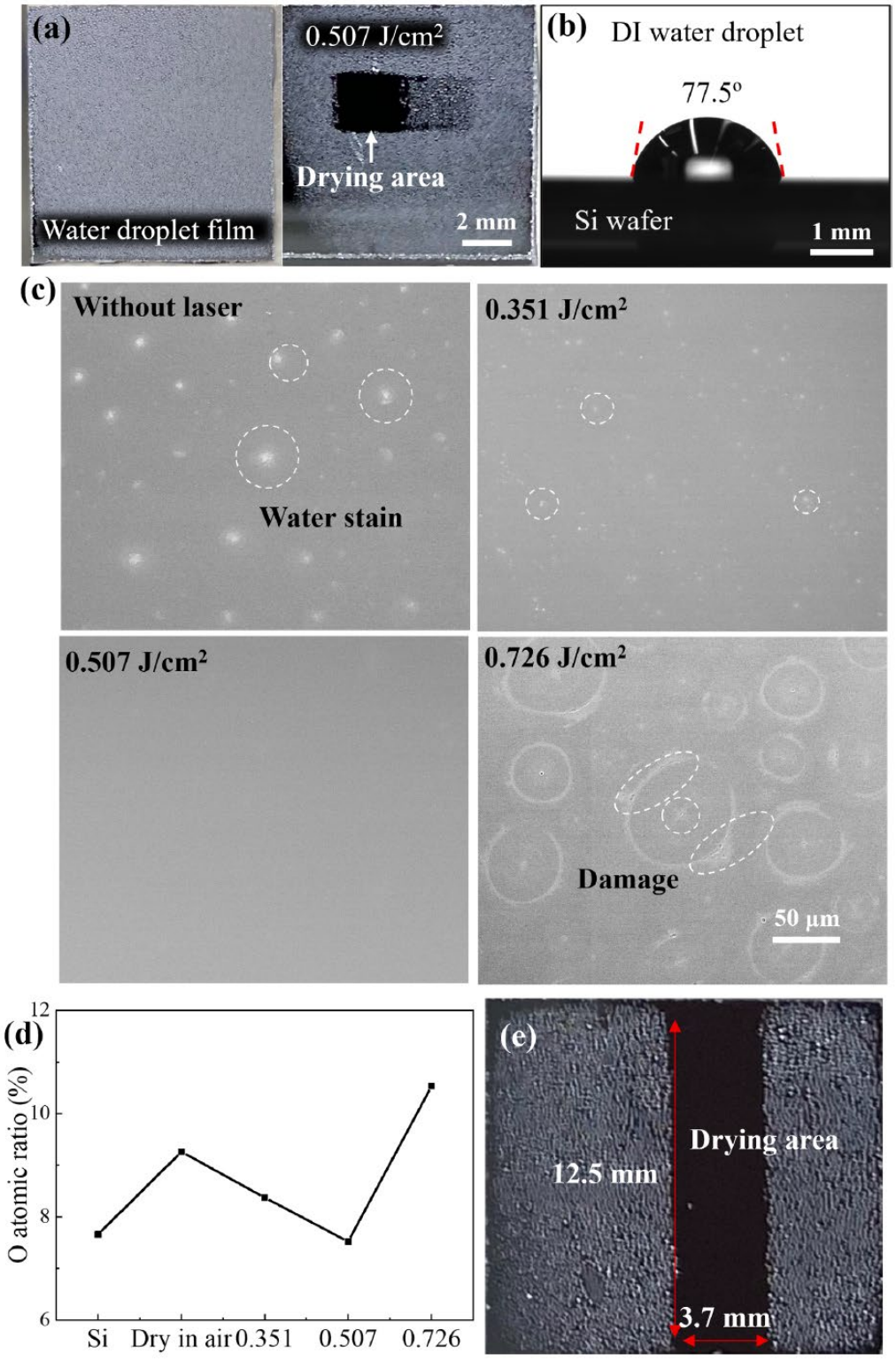


**Fig. 2.** (a) Photographs of the Si wafer (surface oxide layer removed) before and after excimer laser drying. (b) Contact angle measurement of the Si wafer (surface oxide layer removed). (c) SEM images of the Si wafers before and after a single excimer laser pulse at fluences of 0.351, 0.507 and 0.726 J/cm$^2$, respectively. (d) Variation in the O atomic ratio of the controlled and processed surfaces at laser fluences of 0.351, 0.507 and 0.726 J/cm$^2$, respectively. (e) Demonstrated laser drying in a large area (12.5 × 3.7 mm$^2$) using the automated stage.

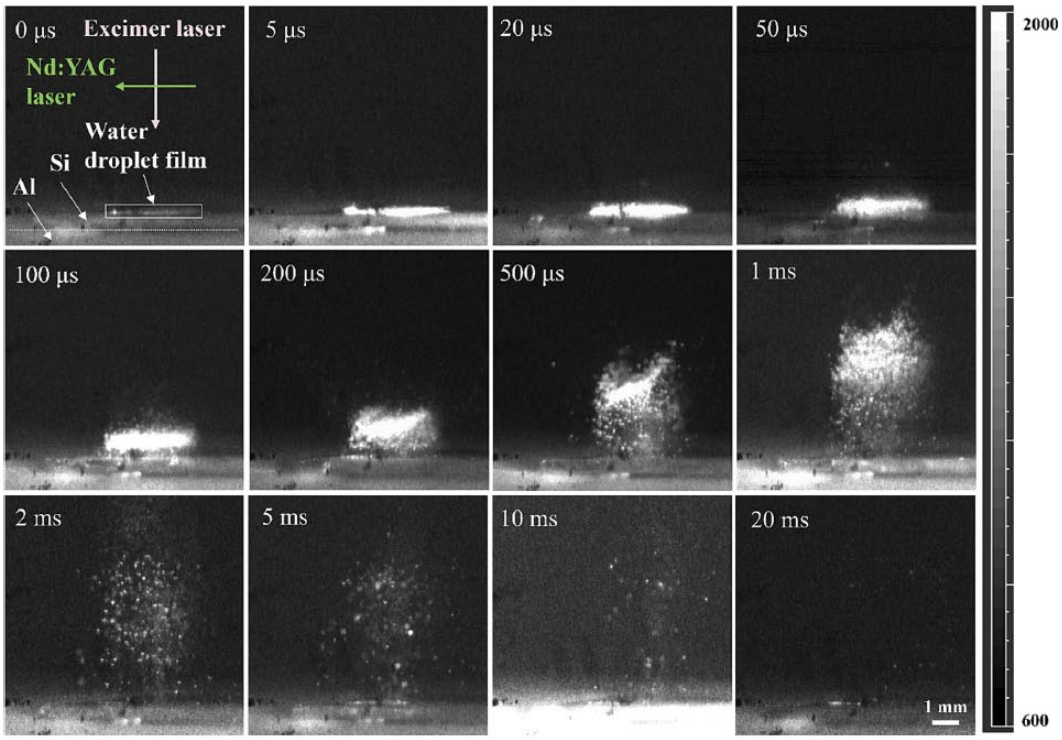


**Fig. 3.** Optical scattering from the ejected water clusters using the Nd:YAG laser at different delays from 0 to 20 ms. The excimer laser was set to a fluence of 0.507 J/cm$^2$. The surface oxide layer of Si wafer was removed.

excimer laser was directed vertically, while the Nd:YAG laser was directed horizontally. The Si wafer with a water droplet film was securely placed on an Aluminum (Al) plate, which was positioned by the automated stage. The excimer laser was set to a laser fluence of 0.507 J/cm$^2$. The scattered green light at 532 nm from the Nd:YAG laser was captured by the ICCD. Fig. 3 shows the laser drying dynamics on a hydrophobic Si wafer, revealing the details starting from the arrival of the excimer pulse to the complete removal of the water droplet films. When the delay was less than 100 μs, the water droplet film became thicker, and the scattered light became stronger. Due to the low absorption coefficient (0.0176 cm$^{-1}$) [38] of water at 248 nm, the excimer laser pulse is primarily absorbed by the Si wafer (absorption coefficient: 1.8064 × 10$^6$ cm$^{-1}$) [39]. Consequently, sub-surface superheating occurs. The heat is transferred to the water droplets, leading to explosive evaporation and the generation of a high vapor pressure [27,28]. The expansion phase lasted for approximately 100 μs, during which the kinetic energy of the expanding water droplets surpassed the surface tension and viscous forces. Then, the water droplets detached from the Si wafer, breaking into small water clusters, which were ejected into the air. It is worth noting that the front clusters acquired similar kinetic

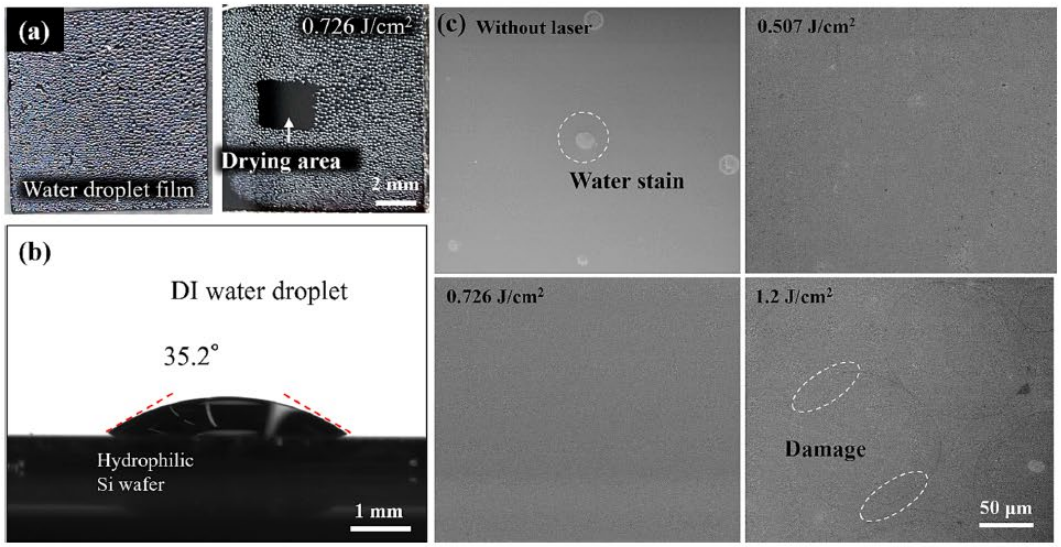


**Fig. 4.** (a) Photographs of the hydrophilic Si wafers (with a native surface oxide layer) before and after excimer laser drying, (b) Contact angle measurement of the hydrophilic Si wafer, (c) SEM images of the hydrophilic Si wafers before and after excimer laser drying at fluences of 0.507, 0.726 and 1.2 J/cm$^2$.

energy and were ejected at a comparable rate. The water ejection process continued for tens of milliseconds, and the water droplet film was completely removed after a delay of 20 ms. Based on the analysis of the water cluster expansion over a time range of 100 μs to 1 ms, the average ejection speed of the water clusters was estimated to be approximately 3.5 m/s.

### 3.3. Laser drying of Si wafers with a native oxide layer

The drying of water on Si wafers with native oxide layers was investigated to examine the influence of hydrophilicity on laser drying. The contact angle of the Si wafer with a native oxide layer was measured to be 35.2°, as shown in Fig. 4**b**, indicating increased hydrophilicity due to the presence of adsorbed hydroxyl groups [33]. For the same volume of water, the water droplet on the hydrophilic Si wafer with oxide is larger and thinner than those on the hydrophobic Si wafer without oxide. Therefore, as shown in Fig. 4**a**, the water droplets deposited appear to be slightly wider than those in Fig. 2**a**. As shown in Fig. 4**c**, the excimer laser with a fluence of 0.507 J/cm$^2$ is unable to remove all the water droplets, resulting in several white stains on the hydrophilic Si surface. In contrast, a clean surface without stains or damage could be achieved on the hydrophobic Si wafer using the same laser fluence. When the laser fluence was increased to 0.726 J/cm$^2$, effective drying on the hydrophilic Si wafer was achieved. However, damage appeared on the hydrophilic wafer when the fluence was further increased to 1.2 J/cm$^2$. As discussed previously, the presence of water droplets can focus the laser and result in a higher effective fluence. The surface hydrophilicity alters the droplet shape, with thinner droplets having smaller curvatures, leading to reduced focusing power. Consequently, a higher laser fluence is required to effectively dry water on hydrophilic Si wafers.

The drying dynamics on the hydrophilic Si wafers (with a native surface oxide layer) at different delays from 0 to 20 ms are shown in Fig. 5. The excimer laser was set to a fluence of 0.507 J/cm$^2$ to study the ejection behavior under the same laser fluence. Similar to the drying process on the hydrophobic Si wafer, the water on the hydrophobic Si wafer underwent the expansion phase before 100 μs, followed by the detachment and ejection phases after 100 μs. However, the water clusters ejected from the hydrophilic Si wafers are significantly larger and more discrete than those on the hydrophobic wafers. By analyzing the water cluster expansion from 100 μs to 1 ms, the average water ejection speed was calculated to be 2.27 m/s, which is slower than that of the hydrophobic Si wafers (the surface oxide layer removed). The lower ejection speed observed on the hydrophilic Si wafer indicates the influence of hydrophilicity on the re-focusing capability of the water droplets deposited. Due to the smaller curvature of the water droplets on the hydrophilic surfaces, the excimer laser experiences a weaker focus than the hydrophobic surface. As a result, the ejection speed of the water droplets is slower when the incident laser fluence is kept the same. Thus, the water droplet film on the hydrophilic surface is not effectively ejected from the surface due to the reduced focusing power, leading to residual water and incomplete drying, as observed in Fig. 4**c**. To compensate for this effect, a higher laser fluence of 0.726 J/cm$^2$ is required for complete drying on the hydrophilic Si surfaces.

### 3.4. The impact of surface roughness on laser drying

The drying dynamics were investigated to explore the impact of surface roughness (textured by fs-laser scanning) on laser drying. Si wafers were textured using a fs laser system, which is detailed in our previous study [40]. The surface morphology of the textured Si wafers is shown in **Figure S5**. The arithmetic mean height (*Sa*) increased from 0.34 to 4.18 μm with an increase in the number of laser scan passes. Specifically, the *Sa* values were obtained for no laser scan, 4, 16, and 48 laser scan passes. The contact angles on the textured Si wafers were around 0° regardless of the number of laser passes. After modification in 1 % vol. FDTS, the contact angles changed to approximately 103° for all the textured and untextured Si wafers. The drying dynamics from 100 μs

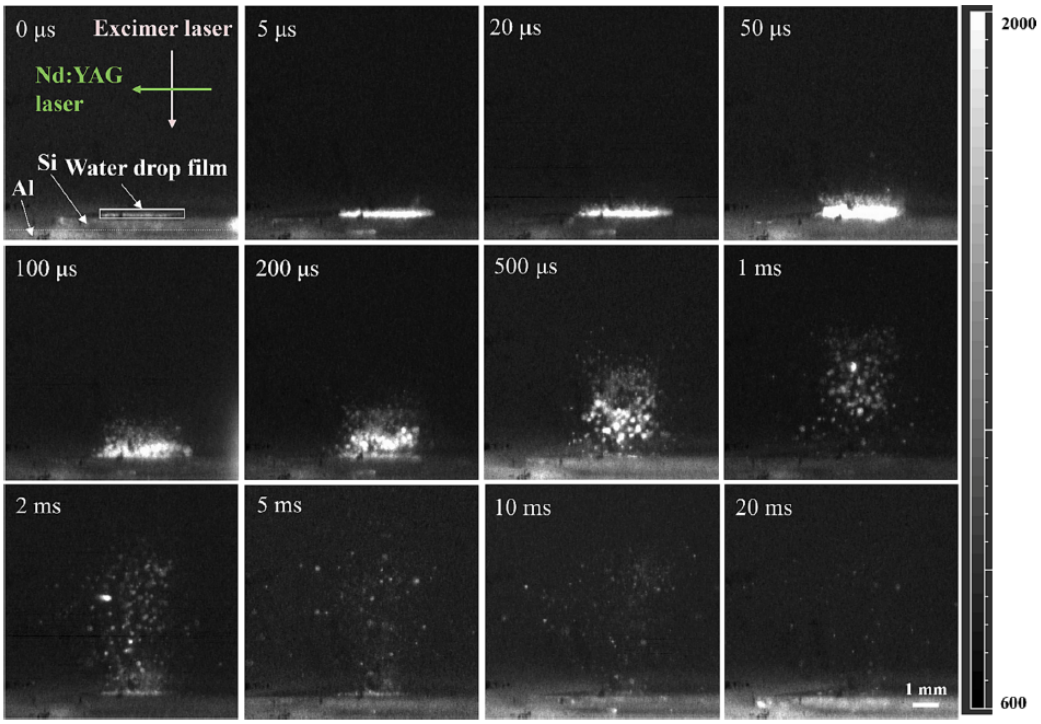


**Fig. 5.** Optical scattering from the ejected water clusters on hydrophilic Si wafers using the Nd:YAG laser at different delays from 0 to 20 ms. The excimer laser was set to a fluence of 0.507 J/cm$^2$. The native surface oxide layer of Si wafer was not removed here.

to 1 ms for the textured Si wafers with different scan passes are shown in Fig. 6. Water droplets detachment from Si surfaces occurs at a delay of around 100 µs, which remains consistent regardless of the surface roughness. However, at a delay of 1 ms, the shape and distribution of the ejected water varied significantly with different roughness. On the untextured Si surface, the ejected water clusters appear as discrete water droplets with diameters of approximately 50 µm. In contrast, on the textured Si surface with 4 scan passes, the ejected water clusters were smaller and denser, and condensed into a mist-like form. As the number of scan passes increased to 16 and 48, discrete droplets appeared along with the mist. This suggests that surface roughness has an impact on the distribution of deposited water and, consequently, the behavior of the ejected water. To note, on the textured Si surface with 4 scan passes, microgrids with a period of 30 µm and a depth of 0.94 µm were fabricated on a Si surfaces, as shown in **Figure S5**. We hypothesize that the deposited water droplet film partially fills the shallow grooves and forms a semi-continuous film as shown in **Figure S6**. In comparison, as the number of scans increased to 16 and 48, the microgrid depths became 7.4 and 15.7 µm, respectively. With these increased depths, **Figure S6** shows that the water droplets reduce in size and are discretely attached along the groove edges. As a result, a discontinuous water film condenses instead of a semi-continuous film, which leads to the formation of a mixture of mist and water clusters.

### *3.5. Laser drying to remove NaCl droplet films*

A 35 g/L NaCl solution was prepared to simulate the conditions of seawater. The contact angle of the 35 g/L NaCl solution on the Si wafer (with the surface oxide layer removed) was measured as 77.8°, very close to that of pure water (77.5°). Fig. 7**a** shows the photographs of the deposited NaCl droplet film on the Si wafer before and after a single pulse of the excimer laser. Here, the native oxide layer was removed on the Si surfaces. It can be observed that the excimer laser pulse with a fluence of 0.507 J/cm$^2$ effectively dried the deposited NaCl droplet film, leaving no stains or damage on the surface (Fig. 7**b**). In contrast, when the solution was left to evaporate in air, stains and NaCl crystals were clearly observed. To investigate the drying dynamics of the NaCl droplet film, time-resolved imaging was used to monitor the droplet film at delays from 0 to 20 ms after the excimer laser pulse with a fluence of 0.507 J/cm$^2$. The detach/ejection phase between 100 µs and 1 ms is shown in Fig. 7**c**. It can be observed that the liquid cluster are ejected at an average velocity of 3.75 m/s, comparable to the average ejection speed for pure water (approximately 3.5 m/s). Interestingly, regardless of the excimer laser fluence, the distribution of the ejected liquid, or the ejection speed, has little difference between the drying of pure water or the 35 g/L NaCl solution. This suggests that the influence of the solution on laser drying is not significant when the concentration is low. Thus, the drying technique demonstrates its ability to dry solutions, such as 35 g/L NaCl, expanding its versatility beyond drying pure water.

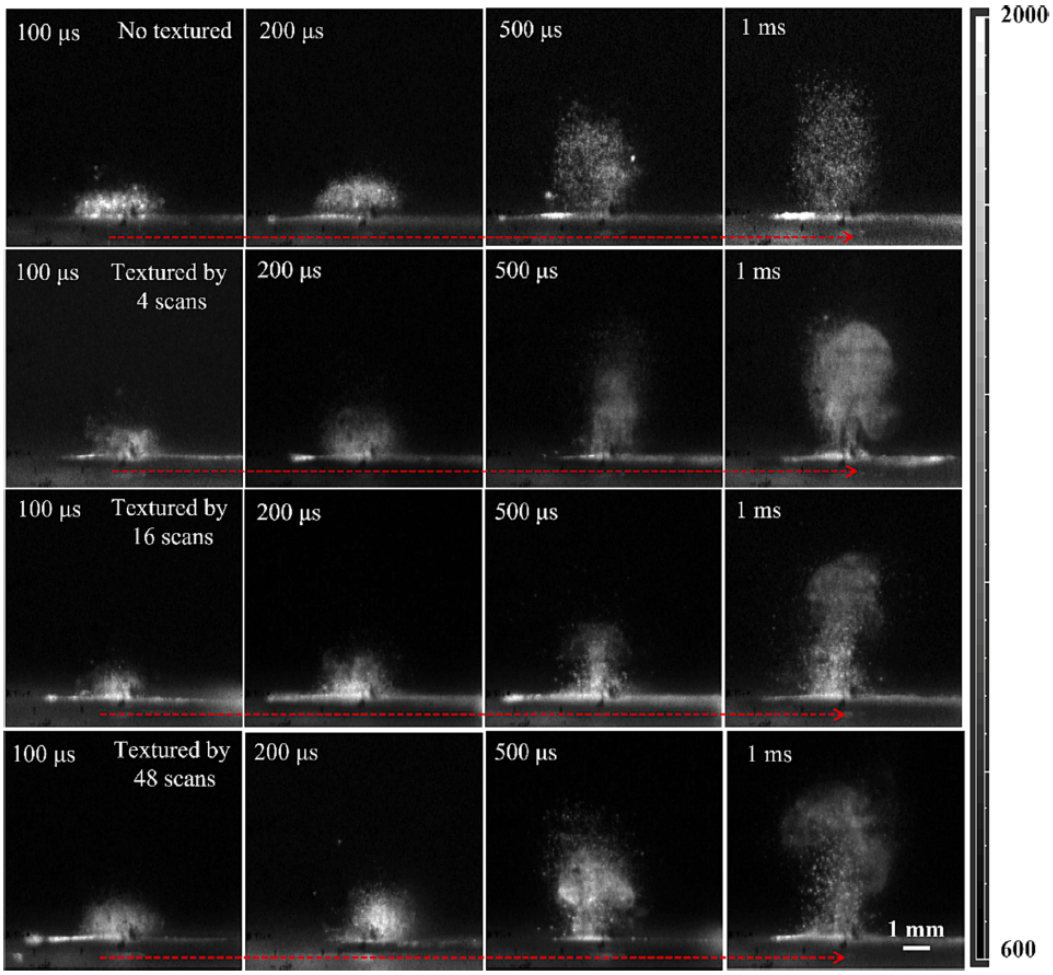


**Fig. 6.** Optical scattering from the ejected water clusters on fs-laser textured Si wafers with no textured, 4, 16, and 48 fs laser scan passes at different delays from 100 µs to 1 ms. The Si surfaces were modified to achieve a contact angle of approximately 103°.

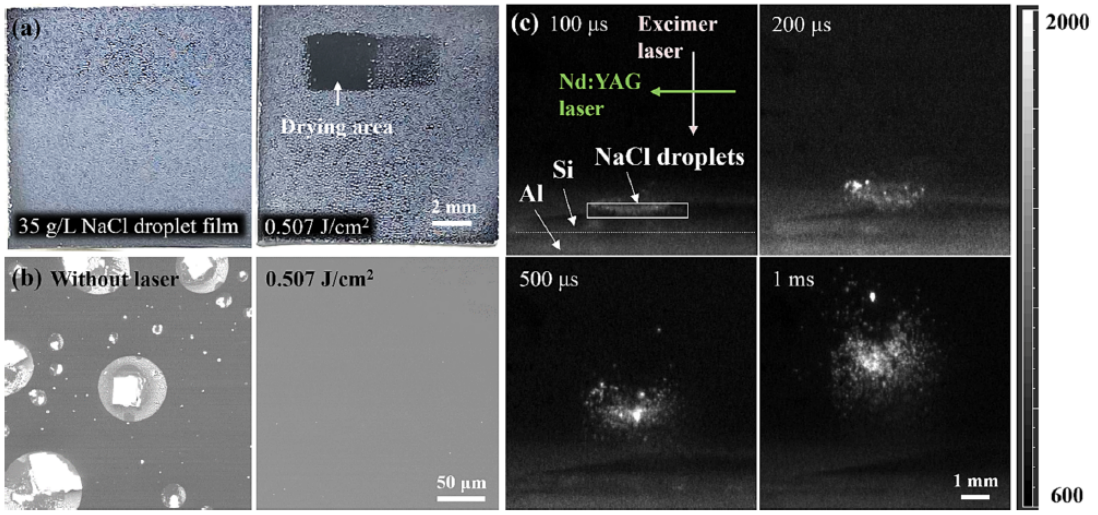


**Fig. 7.** (a) Photographs of a Si wafer before and after drying the 35 g/L NaCl droplet film, (b) SEM images of the Si wafer before and after excimer laser drying at a laser fluence of 0.507 J/cm$^2$, and (c) optical scattering from the ejected NaCl solution from Si wafer at different delays from 100 µs to 1 ms. The surface oxide layer of Si wafer was removed.

### *3.6. Laser drying on polished/mirror polished SS 316 and glass substrates*

The application of the excimer laser for drying water droplet films from other materials was also investigated. Fig. 8**a** presents the photographs of the polished SS 316 substrates after pure water deposition and being dried by a single pulse of excimer laser with a fluence of 0.507 J/cm$^2$. The contact angle of the SS 316 substrates was measured as 43.8°. The surface roughness *Sa* is measured to be 61 nm. The excimer laser pulse with a fluence of 0.507 J/cm$^2$ proved effective in drying the water droplets deposited due to the high absorption coefficient of the SS 316 surface [39] ($8.3691 \times 10^5$ cm$^{-1}$). As shown in the time-resolved images (Fig. 8**c**), the ejected water clusters are large and discrete, similar to those observed on the hydrophilic Si wafers. The average ejection velocity is calculated to be 2.92 m/s.

Mirror polished SS 316 surface (*Sa* = 13 nm) was also investigated by the laser fluence of 0.507 J/cm$^2$, as shown in Fig. 9. The surface profiles of the polished and mirror polished SS 316 substrates are shown in **Figure S7**. The contact angle of the mirror polished SS 316 is 55.5°. From the time resolved imaging, the ejected water clusters show smaller discrete droplets along with the mist (compared to polished SS 316). The ejection speed was calculated to be 3.07 m/s for the mirror polished SS 316. Partial drying of the mirror polished SS 316 was achieved. It is worth noting that the presence of the uncleaned part may be attributed to the weak ghost spot. This also suggests that a higher laser fluence is required for effective drying of mirror polished SS 316, which has a higher reflection than the regularly polished SS 316. The photograph of the complete drying for mirror polished SS 316 by a laser fluence of 1.2 J/cm$^2$ are shown in **Figure S8**. The study demonstrates the capability of the excimer laser in effectively removing liquids from other substrates under different conditions, beyond just Si wafers.

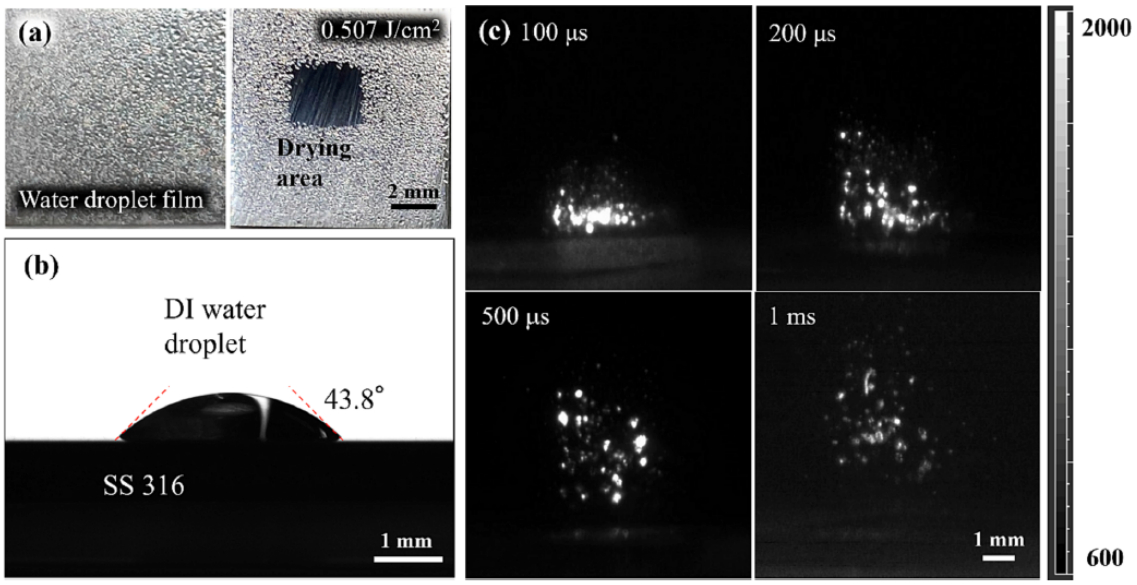


**Fig. 8.** (a) Photographs of the polished SS 316 substrates (*Sa* = 61 nm) before and after excimer laser drying, (b) contact angle measurement of the polished SS 316 substrates, and (c) optical scattering of the ejected water clusters from SS 316 substrates at different delays from 100 µs to 1 ms.

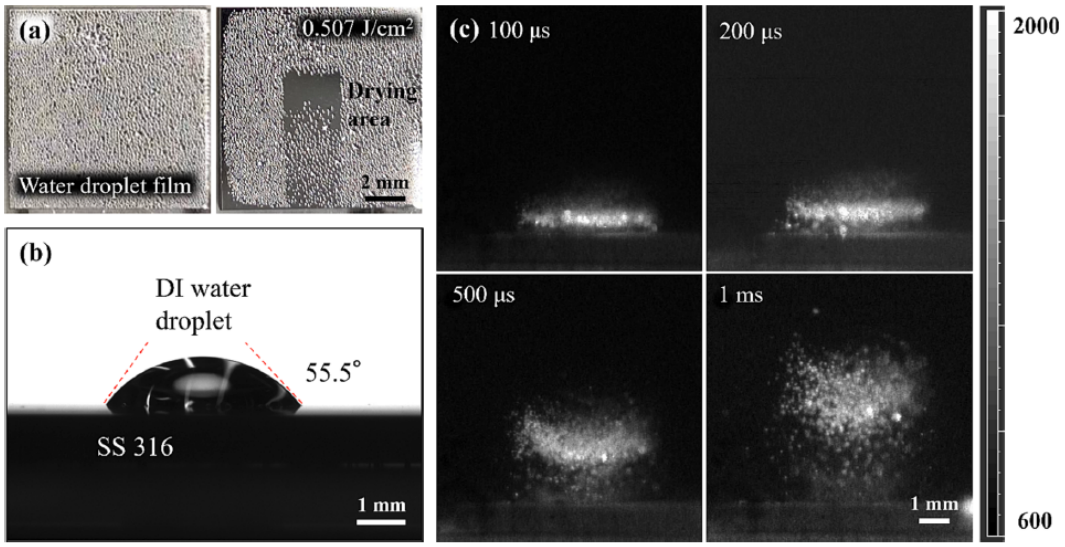


**Fig. 9.** (a) Photographs of the mirror-polished SS 316 substrates ($Sa$ = 13 nm) before and after excimer laser drying, (b) contact angle measurement of the mirror-polished SS 316 substrates, and (c) optical scattering of the ejected water clusters from the mirror-polished SS 316 substrates at different delays from 100 µs to 1 ms.

The laser drying results and dynamics on glass substrates are shown in Fig. 10. The contact angle of the glass substrates was measured to be 52.5°. In contrast to the Si wafers and SS 316 substrates, the excimer laser irradiation had no significant drying effect on pure water droplet films on deposited glass substrates. This can be attributed to the weak optical absorption of the glass [41], which is 1.1983 $cm^{-1}$. When the substrate cannot absorb sufficient energy from the laser, explosive evaporation cannot occur. The water droplet films near the surfaces lack the necessary kinetic energy to overcome surface tension and viscous forces, resulting in unsuccessful drying.

## 4. Conclusions

This study investigated the potential of ns-pulsed laser for surface drying applications. By optimizing the laser fluence to 0.507 J/$cm^2$, clean Si substrates were successfully obtained without any stain or damage. Large-area laser drying was also achieved. The drying results were found to be strongly influenced by the excimer laser fluence, with varying levels of drying effectiveness and potential damage. Time-resolved imaging was employed to investigate the drying dynamics of the ejected water clusters during the laser drying process. It was observed that the deposited water droplet films expand, detach from substrates, and eject into the air after the excimer laser pulses. The shapes of the water droplets, influenced by the surface hydrophilicity, play a significant role in the focusing capability of the ns-pulsed laser. Moreover, the effectiveness of the ns-pulsed laser drying technique was evaluated for different substrates, including stainless steel (polished/mirror polished) and glass. Under the same laser fluence (0.507 J/$cm^2$), the ejection speed of liquid clusters was summarized in Table 1. The overall ejection speed in laser drying can serve as a potential indicator of drying effectiveness, as it signifies the ability of the ejected liquid clusters to overcome surface tension and viscous forces. When the ejection speed reaches a certain threshold (depending on material and surface conditions), it indicates that complete laser drying can been

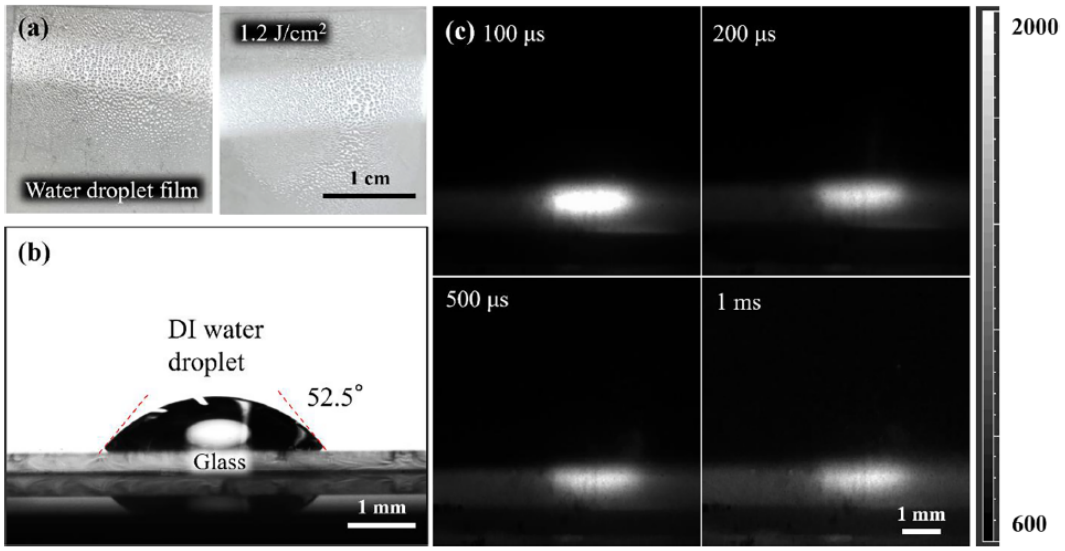


**Fig. 10.** (a) Photographs of the glass substrates before and after excimer laser drying, (b) contact angle measurement of the glass substrate, (c) time-resolved images for laser drying on glass substrates at different delays from 100 µs to 1 ms.

**Table 1**
Summary of drying conditions and ejection speeds.

| Substrate | Surface modification | Liquid | Drying fluence ($J/cm^2$) | Ejection speed (m/s) |
|---|---|---|---|---|
| Si | HF treatment | water | 0.507 | 3.5 (complete drying) |
| Si | No treatment | water | 0.507 | 2.27 (partially drying) |
| Si | HF treatment | 35 g/L NaCl | 0.507 | 3.75 (complete drying) |
| SS 316 | Regular Polish | water | 0.507 | 2.92 (complete drying) |
| SS 316 | Mirror Polish | water | 0.507 | 3.07 (partially drying) |
| Glass | No treatment | water | 1.2 | NA (cannot drying) |

achieved. Moreover, this study demonstrated the ability of the ns-pulsed laser to dry solutions, such as NaCl, in addition to pure water, highlighting its versatility for various substrate and solution types. Overall, the study has shown the potential of the ns-pulsed laser as an environmentally friendly and versatile drying method for diverse applications. Further research is needed to optimize laser parameters and extend the applications of laser drying to other materials and industries where precise and efficient drying is required.

## CRediT authorship contribution statement

**Zhipeng Wu:** Methodology, Data curation, Formal analysis, Investigation, Validation, Writing – original draft, Writing – review & editing. **Xi Huang:** Methodology, Formal analysis, Validation, Writing – original draft, Writing – review & editing. **Wanting Sun:** Methodology. **Haoyu Dong:** Methodology. **Aofei Mao:** Methodology. **Bai Cui:** Resources, Funding acquisition. **Jean-François Silvain:** Resources, Funding acquisition. **Xinwei Wang:** Resources, Conceptualization, Project administration, Supervision, Funding acquisition, Writing – review & editing. **Yongfeng Lu:** Resources, Conceptualization, Project administration, Supervision, Funding acquisition, Writing – review & editing.

## Declaration of Competing Interest

The authors declare that they have no known competing financial interests or personal relationships that could have appeared to influence the work reported in this paper.

## Data availability

Data will be made available on request.

## Acknowledgement

This material is based upon the work supported by the U.S. Department of Energy's Office of Energy Efficiency and Renewable Energy (EERE) under the Advanced Manufacturing Office Award Number DE-EE0009126. The study was also partly performed at the Nano-Engineering Research Core Facility (NERCF), which is partially funded by the Nebraska Research Initiative.

## Appendix A. Supplementary material

Supplementary data to this article can be found online at https://doi.org/10.1016/j.apsusc.2023.158844.

## References

[1] Jin-Goo Park, Michael F. Pas, Effects of drying methods and wettability of silicon on the formation of water marks in semiconductor processing, J. Electrochem. Soc. 1995, 142 (6), 2028.
[2] Wim Fyen, Frank Holsteyns, Twan Bearda, Sophia Arnauts, Jan Van Steenbergen, Geert Doumen, Karine Kenis, Paul W. Mertens, Chapter 19 - A Detailed Study of Semiconductor Wafer Drying, in: Developments in Surface Contamination and Cleaning (Second Edition), Kohli, R.; Mittal, K. L., Eds. William Andrew Publishing: Oxford, 2008; pp 795-854.
[3] A.F.M. Leenaars, J.A.M. Huethorst, J.J. Van Oekel, Marangoni drying: A new extremely clean drying process, Langmuir 6 (11) (1990) 1701–1703.
[4] I.-S. Chang, J.-H. Kim, Development of clean technology in wafer drying processes, J. Clean. Prod. 9 (3) (2001) 227–232.
[5] C. Li, D. Zhao, X. Lu, Experimental Investigation of High-Performance Wafer Drying Induced by Marangoni Effect in Post-CMP Cleaning. *ECS Journal of Solid State*, Sci. Technol. 8 (10) (2019) P557.
[6] J.-G. Park, S.-H. Lee, J.-S. Ryu, Y.-K. Hong, T.-G. Kim, A.A. Busnaina, Interfacial and Electrokinetic Characterization of IPA Solutions Related to Semiconductor Wafer Drying and Cleaning, J. Electrochem. Soc. 153 (9), G811 (2006).
[7] H. Inaba, S. Sakata, T. Yoshida, T. Okada, T. Ohmi, Antistatic protection in wafer drying process by spin-drying, IEEE Trans. Semicond. Manuf. 5 (3) (1992) 234–240.
[8] D.P. Birnie, III; Manley, Manuel, Combined flow and evaporation of fluid on a spinning disk, Phys. Fluids 9 (4) (1997) 870–875.
[9] D.E. Bornside, C.W. Macosko, L.E. Scriven, MODELING OF SPIN COATING, Journal of Imaging Technology 13 (1987) 122–130.
[10] D.E. Bornside, R.A. Brown, P.W. Ackmann, J.R. Frank, A.A. Tryba, F.T. Geyling, The effects of gas phase convection on mass transfer in spin coating, J. Appl. Phys. 73 (2) (1993) 585–600.
[11] H. Mishima, T. Yasui, T. Mizuniwa, M. Abe, T. Ohmi, Particle-free wafer cleaning and drying technology, IEEE Trans. Semicond. Manuf. 2 (3) (1989) 69–75.
[12] H. Mishima, T. Ohmi, T. Mizuniwa, M. Abe, Desorption characteristics of isopropanol (IPA) and moisture from IPA vapor dried silicon wafers, IEEE Trans. Semicond. Manuf. 2 (4) (1989) 121–129.
[13] T. Ohmi, S. Sudoh, H. Mishima, Static charge removal with IPA solution, IEEE Trans. Semicond. Manuf. 7 (4) (1994) 440–446.
[14] Asada, K.; Iwamoto, H.; Hashiguchi, T.; Okamoto, Y.; Minami, T.; Ueno, K.; Kitahara, S. In *A new economical wafer drying technology with high process performance*, 1997 IEEE International Symposium on Semiconductor Manufacturing Conference Proceedings (Cat. No.97CH36023), 6-8 Oct. 1997; 1997; pp E13-E16.
[15] J. Marra, J.A.M. Huethorst, Physical principles of Marangoni drying, Langmuir 7 (11) (1991) 2748–2755.
[16] A. Thess, W. Boos, A model for Marangoni drying, Phys. Fluids 11 (12) (1999) 3852–3855.
[17] O.K. Matar, R.V. Craster, Models for Marangoni drying, Phys. Fluids 13 (7) (2001) 1869–1883.
[18] K. Wolke, B. Eitel, M. Schenkl, S. Rummelin, R. Schild, Marangoni wafer drying avoids disadvantages, Solid State Technology, 1996/08//, 1996,, p. p 87+..
[19] J.T.M. De Hosson, M. De Haas, Analyses of laser and furnace treated sol–gel coatings, Surf. Eng. 14 (5) (1998) 395–399.
[20] Y.-F. Aoyagi, Laser-Induced Dry Cleaning in Air–A New Surface Cleaning Technology in Lieu of Carbon Fluorochloride (CFC) Solvents, Jpn. J. Appl. Phys. 33 (3B) (1994) L430.
[21] Y.F. Lu, M.H. Hong, D.S.H. Chan, T.S. Low, Excimer Laser Applications in Integrated Circuit Packaging, MRS Online Proceedings Library (OPL) 397 (1995) 323.
[22] L. Yue, Z. Wang, W. Guo, L. Li, Axial laser beam cleaning of tiny particles on narrow slot sidewalls, J. Phys. D Appl. Phys. 45 (36) (2012), 365106.
[23] Y.F. Lu, Y.W. Zheng, W.D. Song, Characterization of ejected particles during laser cleaning, J. Appl. Phys. 87 (1) (2000) 549–552.
[24] Y.-F. Lu, W.-D. Song, C.-K. Tee, D. Chan, Siu-Hung; Low, Teck-Seng,, Wavelength Effects in the Laser Cleaning Process, Jpn. J. Appl. Phys. 37 (3R) (1998) 840.
[25] G. Zhu, Z. Xu, Y. Jin, X.i. Chen, L. Yang, J. Xu, D. Shan, Y. Chen, B. Guo, Mechanism and application of laser cleaning: A review, Opt. Lasers Eng. 157 (2022), 107130.
[26] K.M. Smith, M.Y. Hussaini, L.D. Gelb, S.D. Allen, Modeling laser-assisted particle removal using molecular dynamics, Appl. Phys. A 77 (7) (2003) 877–882.
[27] C. Boutopoulos, I. Kalpyris, E. Serpetzoglou, I. Zergioti, Laser-induced forward transfer of silver nanoparticle ink: time-resolved imaging of the jetting dynamics and correlation with the printing quality, Microfluid. Nanofluid. 16 (3) (2014) 493–500.
[28] C. Boutopoulos, M. Chatzipetrou, A.G. Papathanasiou, I. Zergioti, Time-resolved imaging and immobilization study of biomaterials on hydrophobic and superhydrophobic surfaces by means of laser-induced forward transfer, Laser Phys. Lett. 11 (10) (2014), 105603.
[29] L.u. Yong-Feng, Yong-Feng Lu; Shuji Komuro, Shuji Komuro; Yoshinobu Aoyagi, Yoshinobu Aoyagi, Laser-Induced Removal of Fingerprints from Glass and Quartz Surfaces, Jpn. J. Appl. Phys. 33 (8R) (1994) 4691.
[30] Y.F. Lu, W.D. Song, M.H. Hong, D.S.H. Chan, T.S. Low, Theoretical Modeling for Laser Cleaning of Micro-Particles from Solid Surface, MRS Online Proc. Libr. 501 (1) (1997) 399–408.
[31] Y.F. Lu, Y.W. Zheng, W.D. Song, Laser induced removal of spherical particles from silicon wafers, J. Appl. Phys. 87 (3) (2000) 1534–1539.

[32] Y.H. Jin, Y. Zhao, Y. Jiang, Microlens beam homogenizer for excimer laser processing, J. Laser Appl. (2016) 28 (2).
[33] G. Kissinger, W. Kissinger, Hydrophilicity of Silicon Wafers for Direct Bonding, Physica Status Solidi (a) 123 (1) (1991) 185–192.
[34] M. Watanabe, M. Hamano, M. Harazono, The role of atmospheric oxygen and water in the generation of water marks on the silicon surface in cleaning processes, Mater. Sci. Eng. B 4 (1) (1989) 401–405.
[35] G.B. Shinn, F. Steigerwald, H. Stiegler, R. Sauerbrey, F.K. Tittel, W.L. Wilson, Jr.,, Excimer laser photoablation of silicon, J. Vac. Sci. Technol., B: Microelectron. Process. Phenom. 4 (6) (1986) 1273–1277.
[36] K. Hoh, H. Koyama, K. Uda, Y. Miura, Incorporation of Oxygen into Silicon during Pulsed-Laser Irradiation, Jpn. J. Appl. Phys. 19 (7), L375 (1980).
[37] R. Tsu, D. Lubben, T.R. Bramblett, J.E. Greene, Mechanisms of excimer laser cleaning of air-exposed Si(100) surfaces studied by Auger electron spectroscopy, electron energy-loss spectroscopy, reflection high-energy electron diffraction, and secondary-ion mass spectrometry, J. Vac. Sci. Technol. A 9 (2) (1991) 223–227.
[38] Aspnes, D. E.; Studna, A. A., Dielectric functions and optical parameters of Si, Ge, GaP, GaAs, GaSb, InP, InAs, and InSb from 1.5 to 6.0 eV. *Physical Review B* **1983**, *27* (2), 985-1009.
[39] P.B. Johnson, R.W. Christy, Optical constants of transition metals: Ti, V, Cr, Mn, Fe Co, Ni, and Pd, Phys. Rev. B 9 (12) (1974) 5056–5070.
[40] N. Li, X.i. Huang, H. Dong, B. Duan, Q. Zhu, A. Mao, P. Li, B. Cui, J.-F. Silvain, Y. Lu, Gold-coated nanoripples produced by UV-Femtosecond lasers for surface enhanced Raman spectroscopy, Appl. Surf. Sci. 636 (2023), 157794.
[41] Refractive index of BK7 - SCHOTT.